D6-23872
March 1969

The Effect of Silicon on the Stress Corrosion Resistance of Low-Alloy, High-Strength Steels

by
C.S.Carter

BOEING COMMERCIAL AIRPLANE DIVISION
Renton, Washington

Sponsored by
Advanced Research Projects Agency
ARPA Order No. 878

THE EFFECT OF SILICON ON THE STRESS CORROSION RESISTANCE OF LOW-ALLOY, HIGH-STRENGTH STEELS*

By C. S. Carter†

ABSTRACT

The effect of five levels of silicon, within the range 0.09% to 2.15%,§ on the stress corrosion resistance of 4340 steel was established in 3.5% sodium chloride solution for two tensile strength ranges (280 to 300 ksi and 230 to 240 ksi). At the higher strength range, the threshold stress intensity K_{Iscc} was independent of silicon content, but the stress corrosion crack velocity was significantly retarded when the silicon content exceeded 1.5%. At the 230- to 240-ksi strength range, steels containing less than 1.5% silicon exhibited a higher K_{Iscc} threshold than steels of higher silicon content. Strength level had a significant effect on crack velocity characteristics.

INTRODUCTION

Low-alloy steels, quenched and tempered to tensile strength levels up to 300 ksi, are employed in a number of structural components. To achieve this strength level, the alloys contain about 0.4% carbon with other elements added to obtain hardenability and tempering resistance. In the past, 4340 (260- to 280-ksi tensile strength range) has been used extensively for such components but, more recently, a modified version of 4340 (designated 300M) has been used in the range 270 to 300 ksi. The 300M alloy contains 1.5% to 1.8% silicon and 0.1% vanadium, whereas the silicon content of 4340 is 0.2% to 0.35% and vanadium is not added. The silicon was added to increase the tempering resistance, thereby allowing a higher tempering temperature than with 4340 and so providing a greater degree of stress relief. These modifications also provided a higher strength level than could be guaranteed with 4340 (1,2).

Service experience with 300M alloy has been extremely good, but some failures of components fabricated from 4340 have been reported (3,4). In most cases, the failure was attributed to the development of stress corrosion cracks and subsequent brittle fracture of the component. Because of this difference in service performance, the question arises–does silicon enhance the stress corrosion resistance of 4340-type steels, or is the superior service performance of 300M attributable to some other effect, for example, the greater degree of stress relief? Furthermore, if silicon improves the stress corrosion resistance, does the range 1.5% to 1.8% represent the optimum level? The aim of this investigation was to answer these questions.

Five experimental heats of 4340 having different silicon contents were prepared and the stress corrosion characteristics determined for two tensile strength ranges (280 to 300 ksi and 230 to 240 ksi). In addition, samples from large heats of 4340 and 300M were compared. The stress corrosion resistance was evaluated using a fracture mechanics approach in order to study the influence of crack tip stress intensity upon the individual crack extension mechanisms involved in complete failure.

MATERIALS

EXPERIMENTAL HEATS

A single heat of 4340 was air melted and split into five separate 100-lb heats, and the desired level of silicon was added to each. These were then cast into electrodes, consumable vacuum remelted, and hot rolled to 1-1/2-in.-square bar.

* This research was supported by the Advanced Research Projects Agency of the Department of Defense (ARPA Order No. 878) under Contract N00014-66-C0365.

† The author is associated with the Commercial Airplane Division of The Boeing Company, Renton, Washington.

§ All material percentages in this paper are weight percentages.

Table I. Alloy composition.

Heat	Alloy	Melting practice	Form	Chemical analysis									ASTM grain size no.[a]
				C	Mn	S	P	Si	Cr	Mo	Ni	V	
	Experimental												
A	4340 + 0.09% Si	CEVM	1½-in.-sq bar	0.43	0.80	0.006	0.006	0.09	0.89	0.28	1.86	–	6
B	4340 + 0.54% Si	CEVM	1½-in.-sq bar	0.43	0.79	0.006	0.006	0.54	0.89	0.28	1.87	–	8
C	4340 + 1.08% Si	CEVM	1½-in.-sq bar	0.44	0.77	0.006	0.006	1.08	1.01	0.26	1.85	–	7
D	4340 + 1.58% Si	CEVM	1½-in.-sq bar	0.43	0.68	0.006	0.004	1.58	1.05	0.26	1.84	–	6
E	4340 + 2.15% Si	CEVM	1½-in.-sq bar	0.43	0.68	0.006	0.004	2.15	1.07	0.26	1.84	–	5
	Commercial												
F	4340	Air melt	8- by 8-in. billet	0.40	0.70	0.019	0.021	0.21	0.86	0.26	1.86	–	Not measured
G	4340	Vacuum degassed	8-in. round	0.40	0.73	0.013	0.014	0.28	0.87	0.25	1.80	–	Not measured
H	300M	CEVM	5- by 5-in. billet	0.41	0.87	0.008	0.007	1.69	0.86	0.10	1.78	0.07	Not measured
J	300M	CEVM	4- by 4-in. billet	0.43	0.90	0.003	0.010	1.57	0.78	0.37	1.78	0.09	Not measured

[a]Prior austenite grain size.

The chemical analysis of these heats is shown in Table I. The sulfur and phosphorus contents of these heats were restricted to a maximum level of 0.01% since previous work has shown that these elements have a detrimental influence on fracture toughness (5,6).

COMMERCIAL HEATS

Two heats of 4340, one air melted and the other vacuum degassed, were obtained in billet form. Two heats of 300M, prepared by consumable electrode vacuum remelting, were also acquired. The chemical analysis of these alloys is also shown in Table I.

EXPERIMENTAL PROCEDURE

EXPERIMENTAL HEATS

To determine the tempering temperatures necessary to achieve the desired tensile strength ranges, a preliminary tempering study was conducted on each heat. Tensile specimens of 0.25 in. diameter were machined in the longitudinal direction from the bar stock. These were normalized at 1650°F for 1 hr, austenitized at 1600°F for 1 hr, oil quenched and tempered for 2 hr, plus 2 hr at temperatures within the range 400° to 1000°F. The mechanical properties were subsequently determined at room temperature and at a strain rate of 0.005 in./in./min.

Single-edge-notched specimens (Fig. 1) were machined in duplicate from the bars in the longitudinal direction. These were heat treated as described above, tempered to the desired strength level, ground to final dimensions, and fatigue precracked. The plane strain fracture toughness K_{Ic} was determined by loading the specimens in four-point bending, and the results were analyzed according to the recommended ASTM procedure (7). Duplicate tensile specimens were subsequently machined from the broken halves of the notched bend specimens and tested as described above.

To evaluate stress corrosion resistance, the fatigue cracked notched bend specimens were hydraulically sustain loaded to selected initial stress intensity K_{Ii} levels in cantilever bending using the procedure described by Brown (8,9). Just before

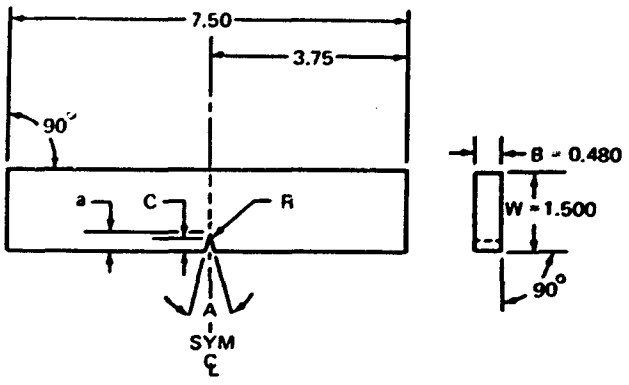

A = 45° NOTCH ANGLE
R = 0.011 MAX NOTCH RADIUS
C = 0.225 ± 0.001 NOTCH DEPTH
a = NOTCH DEPTH PLUS AVERAGE FATIGUE CRACK DEPTH
B = 0.480 ± 0.001–SPECIMEN THICKNESS
W = 1.500 ± 0.001–SPECIMEN WIDTH

ALL DIMENSIONS IN INCHES

Fig. 1. Notched bend specimen.

each specimen was loaded, 3.5% aqueous sodium chloride solution was dripped into the notch through a plastic spigot from a reservoir containing the solution. The specimens were exposed to the continued flow of the solution until failure occurred or until a selected time period elapsed. A graduated scale was attached to certain specimens and the length of the stress-corrosion crack measured by optical observation at selected time intervals. From this data, a crack length versus time curve could be constructed. The slope of the curve, which represents the instantaneous crack growth rate, was graphically determined for various crack length values and the relationship between stress intensity (Eq 1) and crack velocity determined.

Specimens which remained unbroken were either fatigue cracked again and retested or treated as fracture toughness specimens and loaded to failure in air. In either case, the region under the fatigue crack was subsequently examined by optical means for evidence of environmental crack growth. The time-to-failure was recorded for the specimens which failed during testing, and the extent of environmental crack growth was measured. Since the applied load was constant, the stress intensity level $K_{I\delta}$ at which rapid mechanical failure was initiated from the tip of the stress corrosion crack could be determined.

The applied stress instensity was determined from the expression:

$$K = \frac{6Ma^{1/2}Y}{bW^2} \qquad (1)$$

where M = bending moment
b = specimen thickness
W = specimen width
a = notch depth plus average fatigue crack depth
Y = a factor depending upon the ratio of a:W and the loading system employed

Since values for Y have not been rigorously determined for cantilever bending, the polynomial relationship established by Brown and Srawley (7) for specimens loaded in three-point bending with a loading span to width ratio of 8 to 1 was used.

COMMERCIAL HEATS

Tensile specimens of 0.25-in. diameter and surface-flawed specimens (Fig. 2) were machined from the longitudinal direction of billets F, G, and H. Notched bend specimens (Fig. 1) were machined at similar locations from billet J. The 4340 specimens were normalized at 1625°F, austenitized at 1525°F, oil quenched, and double tempered at 400°F. The 300M specimens were similarly treated except that the temperatures were 1650° 1600° and 600°F, respectively. All specimens were ground to final dimensions after heat treatment. A 0.140-in.-deep notch was electrodischarge machined into the surface-flawed specimens and subsequently sharpened by fatigue cracking prior to testing.

The tensile tests were conducted in the same manner as described for the experimental heats.

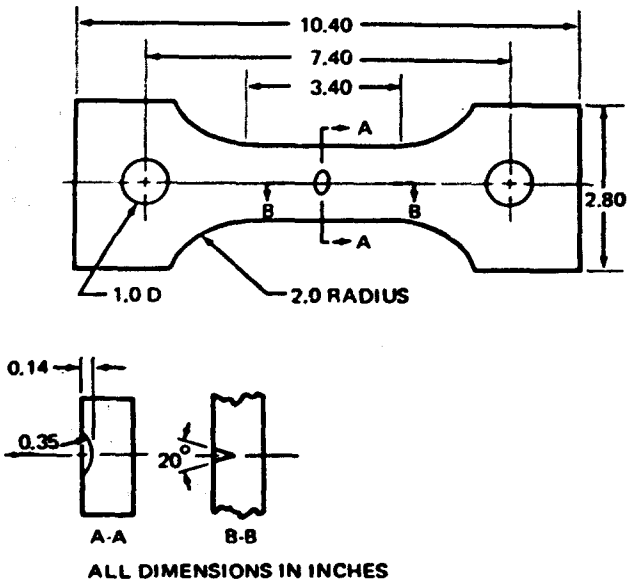

Fig. 2. Surface-flawed specimen.

The surface-flawed specimens were loaded in tension in high-humidity air; a relative humidity of greater than 85% (70°F) was produced by bubbling bottled air through room temperature water. Three types of test were used to evaluate the influence of this environment on heats F through H:

1. Fracture Toughness Tests–These were conducted in tension at a loading rate of 150 ksi/min. Fracture of the specimens typically occurred after less than 1 min of loading. Fracture toughness K_{Ic} was determined from the surface flaw stress intensity solution given by Irwin (10).
2. Sustained Load Tests–These were accomplished by initially loading the specimens to 90% of the K_{Ic} value. Specimens that survived this stress intensity for several hours were subsequently step loaded and held at higher loads until failure occurred. In addition, specimens were held in the range 30% to 45% of K_{Ic} for several hours. Subsequent fatigue cracking in dry air (less than 10% relative humidity) at 120 cpm and at a stress ratio of 0.05 defined the extent of growth; specimens were then tested in a similar way to the fracture toughness specimens.
3. Fatigue Tests–To evaluate the effects of environment on fatigue crack growth, fatigue cracked specimens were subjected to slow cyclic rates (5 cpm) and at a stress ratio of 0.8. The specimens were then cycled again in dry air and broken as described above (in 2).

A fractographic examination was conducted on all the broken specimens.

The stress corrosion resistance of the other 300M billet (heat J) was evaluated using precracked notched bend specimens as described for the experimental alloys.

RESULTS AND DISCUSSION

EXPERIMENTAL HEATS

The mechanical property data obtained over the tempering range exhibited characteristics similar to those previously reported for comparable steels (1,11) and therefore are not discussed here. The tempering temperatures selected for the two strength ranges in each heat are shown in Table II, together with the mechanical properties obtained

Table II. Mechanical properties of experimental alloys[a].

Heat	Tempering Temperture (°F)	Tensile strength (ksi)	Yield strength (ksi)	Elongation (%)	Reduction of area (%)
	280- to 300-ksi strength range				
A	400	284.2	201.8	11	32
B	400	299.2	216.5	12	39
C	500	290.5	240.0	12	40
D	500	291.3	236.4	11	39
E	500	297.4	240.7	10	35
	230- to 240-ksi strength range				
A	600	239.9	204.2	10	34
B	750	228.5	201.4	11	43
C	800	231.1	193.8	11	40
D	850	236.6	196.6	11	36
E	925	240.2	215.8	10	33

[a]Mean of duplicate tensile tests.

by these treatments. In all cases except one, the tensile strength levels were within the desired ranges of 280 to 300 and 230 to 240 ksi. The exception was the 0.54% silicon heat in which the tensile strength level of 228 ksi was slightly outside the required limit. It should be noted that, in the higher strength range, the tempering temperatures selected did not necessarily produce the maximum yield strength. These temperatures were selected to provide the best overall correspondence of yield strength, ultimate strength, and tempering temperature among the five heats.

As shown in Fig. 3, there was no improvement in the fracture toughness of the higher strength alloys as the silicon content was increased from 0.54% to 2.15%. The K_{Ic} values of 50 to 55 ksi$\sqrt{in.}$ are typical of 4340 but are lower than those reported for 300M (12). Reducing the silicon content to 0.09% increased K_{Ic} by 40%.

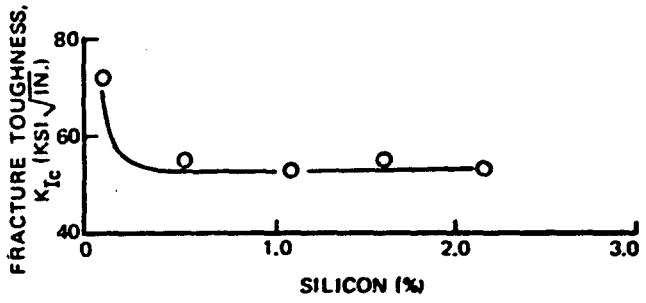

Fig. 3. Effect of silicon on K_{Ic} (280- to 300-ksi strength range).

Decreasing the strength from 280-300 ksi to 230-240 ksi led to an improvement in fracture toughness in all the alloys except the one containing 2.15% silicon (Fig. 4). The K_{Ic} value for the latter steel was similar to that obtained in the higher strength range.

Stress corrosion curves of K_{Ii} versus time to failure were established, typical examples of which are shown in Fig. 5, and the threshold stress intensity K_{Iscc} below which stress corrosion cracking did not occur was determined.

As shown in Fig. 6, the K_{Iscc} of all the steels heat treated to the 280- to 300-ksi strength range were between 13 and 16 ksi$\sqrt{in.}$. Therefore, silicon does not enhance the threshold stress intensity level. Reducing the strength level significantly improved the K_{Iscc} in the steels containing less than 1.5% silicon; the higher silicon content steels showed only a slight improvement (Fig. 7). The low K_{Iscc} value recorded for the 0.09% silicon heat can be attributed to the lower tempering temperature used for this steel.

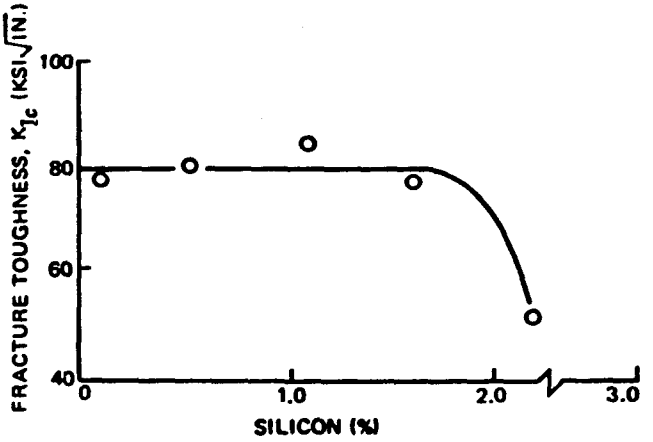

Fig. 4. Effect of silicon on K_{Ic} (230- to 240-ksi strength range).

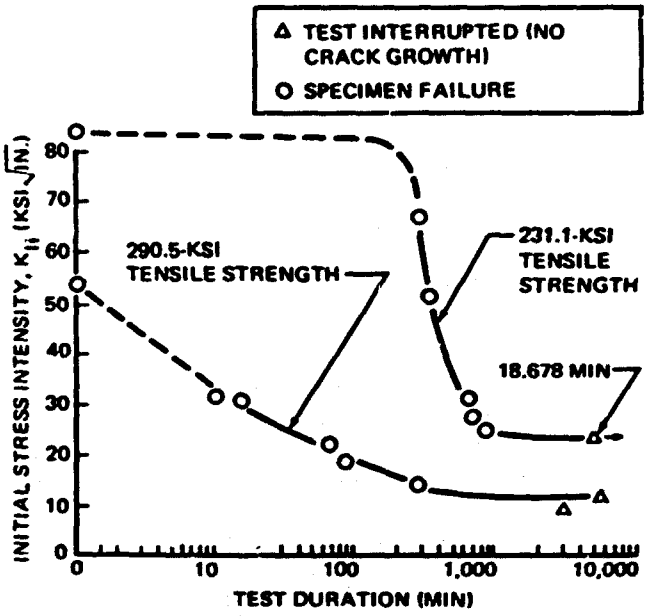

Fig. 5. Stress corrosion curves for 1.08% silicon steel.

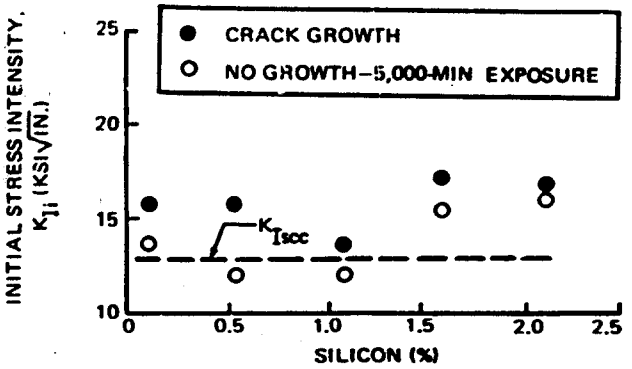

Fig. 6. Effect of silicon on threshold stress intensity K_{Iscc} (280- to 300-ksi strength range).

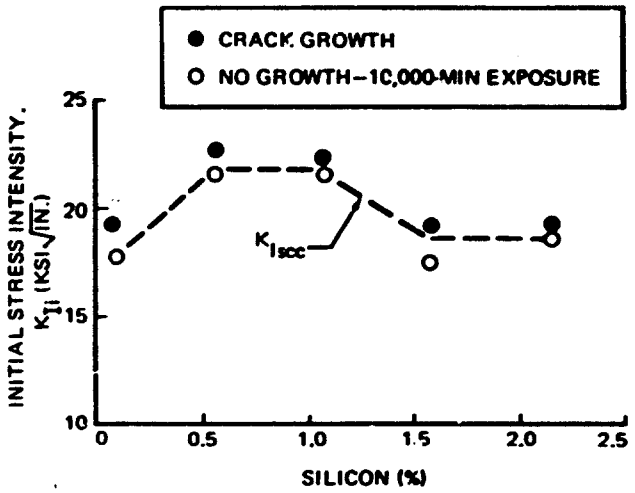

Fig. 7. Effect of silicon on threshold stress intensity K_{Iscc} (230- to 240-ksi strength range).

Crack length versus time curves were obtained from specimens loaded initially to a K_{Ii} of approximately 30 ksi$\sqrt{in.}$; typical curves are shown in Figs. 8 and 9. In these tests, it was observed that an incubation time was required before crack growth was initiated. An attempt was made to obtain a measure of this period oy extrapolating to the time required for the initial 0.01 in. of crack extension. This showed some scatter but indicated that silicon had no effect on the incubation period at either strength level. However, decreasing the strength level generally increased the incubation time from a few minutes to approximately 1 hr.

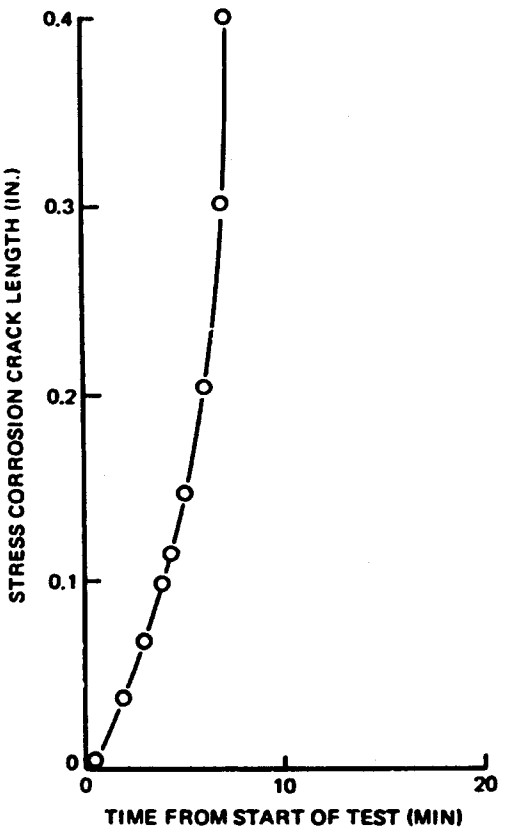

Fig. 8. Crack growth characteristics for 0.09% silicon steel (284.2-ksi tensile strength).

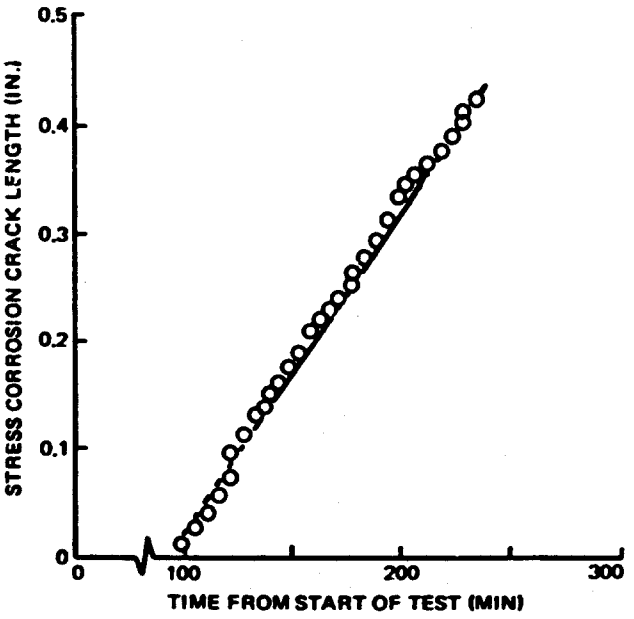

Fig. 9. Crack growth characteristics for 0.54% silicon steel (228.5-ksi tensile strength).

The effect of stress intensity level on stress corrosion crack growth rate is shown in Fig. 10 for the 280- to 300-ksi strength range. The data indicate that the growth rate was directly proportional to the stress intensity; a similar relationship has been reported by other investigators for 4340 (13) and H11 steels (14). Silicon had a significant effect on the crack growth rate over the range of stress intensity level examined. Steels with silicon contents of 0.09%, 0.54%, and 1.08% had similar growth rates, and the data points could be enclosed within the same scatter band. There was, however, a marked retardation in crack growth rate when the silicon content was increased to 1.58%, and a further decrease occurred on increasing the silicon content to 2.15%. This decrease in crack growth rate is also reflected by the time to failure at a K_{Ii} of 32 ksi$\sqrt{in.}$, which increased at silicon levels above 1.08% (Fig. 11).

The kinetics of crack growth for the steels tempered to the 230- to 240-ksi strength range were significantly different from those at the higher strength range. The growth rate was generally much slower than in the higher strength range and was constant over a wide range of stress intensity. The range of stress intensity over which the crack growth rate was found to be constant, and the growth rates, are shown in Table III. This phenomenon was also reflected in the K_{Ii} versus time to failure for the lower strength steels since there was only a slight dependence of failure time on K_{Ii} (Fig. 5).

Table III. Crack velocity in 230- to 240-ksi tensile strength steels.

Heat	Stress intensity range over which constant crack velocity was measured (ksi $\sqrt{in.}$)	Crack velocity (constant) (in./min)
A	31.6 to 53.0*	0.01
B	31.5 to ~K_{Ic}	0.0025
C	31.0 to ~K_{Ic}	0.001
D	27.6 to ~K_{Ic}	0.0025
E	31.5 to 43.7*	0.005

*Velocity directly proportional to K when stress intensity exceeded this limit.

NOTE: Lower end of range corresponds to K_{Ii}

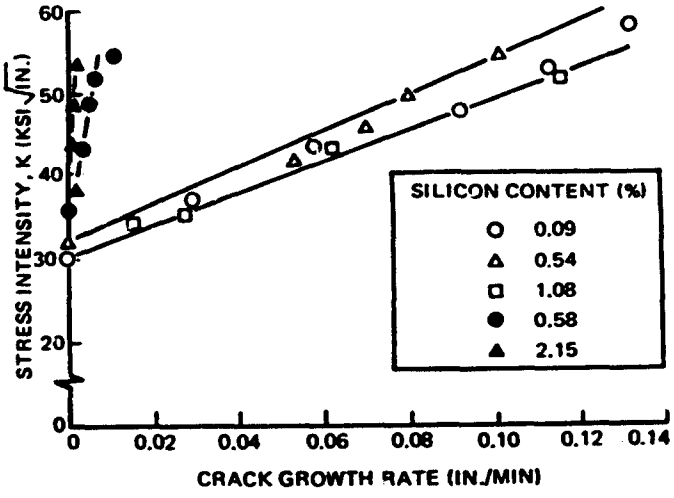

Fig. 10. Influence of silicon content on stress corrosion crack growth rate (280- to 300-ksi strength range).

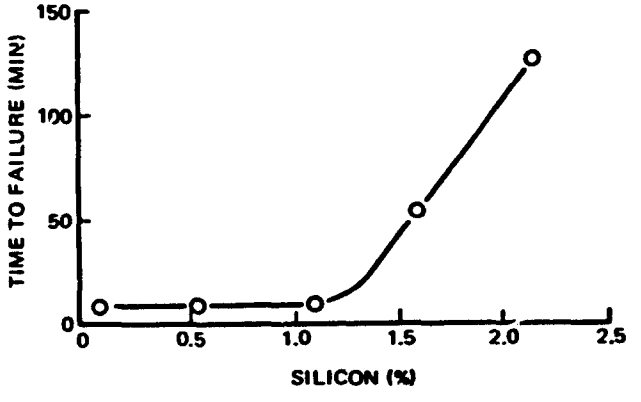

Fig. 11. Effect of silicon content on time to failure at K_{Ii} of 32.0 ksi $\sqrt{in.}$ (280- to 300-ksi strength range).

The critical stress intensity level $K_{I\delta}$ for brittle fracture initiation from the tip of the extending stress corrosion crack is shown in Table IV. In many tests, the critical crack length (plus notch depth) divided by the specimen width exceeded 0.6, which is the limit for the expression used (Eq 1). Under these circumstances, $K_{I\delta}$ is shown in Table IV as greater than the limiting K value. The data indicated that, at both strength levels, $K_{I\delta}$ was significantly greater than K_{Ic}; similar data have been reported for other high-strength steels (15). There was no apparent effect of silicon on

Table IV. Critical stress intensity for rapid brittle failure.

Heat	$K_{I\delta}$ Values for individual specimens (ksi$\sqrt{in.}$)	K_{Ic} (ksi$\sqrt{in.}$)
	280- to 300-ksi strength range	
A	> 47.4: > 67.0: > 96.2: > 93.0: > 38.4	74.2
B	> 64.0: > 49.0: 74.0: 79.0	55.0
C	66.0: > 55.0: > 40.5: > 69.0: 73.5	53.8
D	> 64.0: 63.0: 81.5: > 48.7: 89.5	55.2
E	> 61.6: > 50.5: > 96.5	51.9
	230- to 240-ksi strength range	
A	> 93.0: > 63.8: > 96.0: > 96.0: > 64.0: > 44.5	78.3
B	> 94.5: 128: > 82.5: > 67.0: > 77.0	80.7
C	> 74.8: > 77.2: 126: 126: > 94.5: 142	85.3
D	> 64.0: 159: > 86.5: > 94.5: > 57.8: > 54.6	76.6
E	62.0	51.9

this behavior. In the lower strength range, this blunting effect could be definitely associated with the tendency of the stress corrosion crack to branch; branching was observed in all the heats except that with the highest silicon content. Specimens tempered to the 260- to 280-ksi strength range did not exhibit branching. Therefore the blunting effect, which was less severe than in the lower strength steels, must be associated with other phenomena. Possibly the intergranular mode of crack extension and local deviations from the notch plane along the crack front led to the effect.

Fracture toughness K_{Ic} values were determined for those specimens which had been loaded to stress intensity levels below K_{Iscc} in the sodium chloride solution and subsequently broken open (Table V). These values corresponded to the K_{Ic} determined from a sharp unexposed fatigue crack, suggesting that immersion in salt did not blunt the fatigue crack tip. It must be remembered, however, that crack blunting only becomes apparent below a certain stress intensity level determined by the yield strength and crack acuity (16). Therefore, although blunting was not apparent in the K_{Ic} range of 50 to 80 ksi$\sqrt{in.}$, it is possible that such an effect may have existed at lower stress intensity levels, for example, close to K_{Iscc}.

COMMERCIAL HEATS

The mechanical properties of the materials are shown in Table VI. Fractographic examination of the region immediately below the fatigue precrack in the air-melted fracture toughness specimens revealed that intergranular cracking (0.03-in. length) preceded the final dimple rupture fracture. The vacuum degassed material

Table V. Effect of immersion below K_{Iscc}.

Heat	Strength range (ksi)	Initial stress intensity K_{Ii} (ksi$\sqrt{in.}$)	Immersion time in 3.5% sodium chloride solution (min)	Critical stress intensity after immersion, K_{Ic}' (ksi$\sqrt{in.}$)	$\frac{K_{Ic}'}{K_{Ic}}$
A	280-300	12.0	7,038	76.5	1.03
A	230-240	23.4	25,942	72.2	0.93
B	280-300	13.6	4,190	52.5	0.96
E	230-240	16.0	10,020	46.4	0.90

Table VI Mechanical properties of commercial alloys.

Heat	Alloy	Melting practice (ksi)	Tensile strength (ksi)	Yield strength (ksi)	Elongation (%)	Reduction of area (%)	K_{Ic} (ksi$\sqrt{in.}$)
F	4340	Air melt	271.2	212.2	12	49	63.0
G	4340	Vacuum degassed	271.6	220.8	12	45	63.6
H	300M	CEVM	291.1	247.0	8	37	73.9
J	300M	CEVM	301.9	251.5	11	38	63.5

exhibited a similar topography, although the extent of intergranular cracking was less. Heat H (300M) showed no tendency toward intergranular failure: the transition from transgranular fatigue to dimple rupture was sharply defined.

Results of the sustained load testing are shown in Figs. 12 and 13. The 4340 air-melted material failed almost immediately when loaded to a stress intensity equal to 90% of K_{Ic}. Vacuum degassed 4340 and the 300M survived 90% of K_{Ic} for periods up to 6 hr, although crack growth occurred in the 4340 steel. Subsequent step loading resulted in failure at 96% of K_{Ic}. Fractographic examination revealed that initial growth in the 4340 steels occurred in an intergranular manner, but this was absent from the 300M specimens. Testing at lower stress intensity levels (43% of K_{Ic}) showed the 4340 air-melted material to be susceptible to stable crack extension under sustained load. At comparable stress intensity levels, no growth was apparent in the 300M steel.

Fatigue cycling of the 4340 air-melted steel at an initial stress intensity level equal to 43% of K_{Ic} revealed crack extension in less than 500 cycles. In similar tests on 300M at stress intensity levels of 34%, 70%, and 80% of K_{Ic}, no cracking occurred after 500 cycles. Fractography revealed that a wet environment was required for intergranular propagation since the fracture mode changed from intergranular to transgranular as the environment changed from wet to dry.

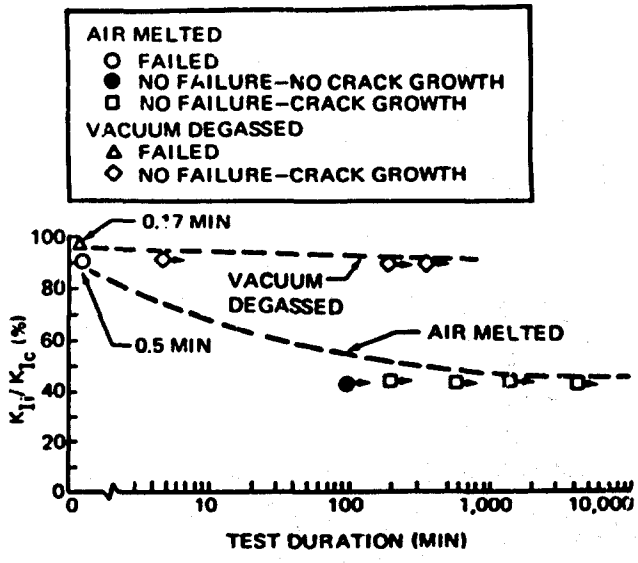

Fig. 12. Commercial alloy 4340 tested in 90% relative humidity air.

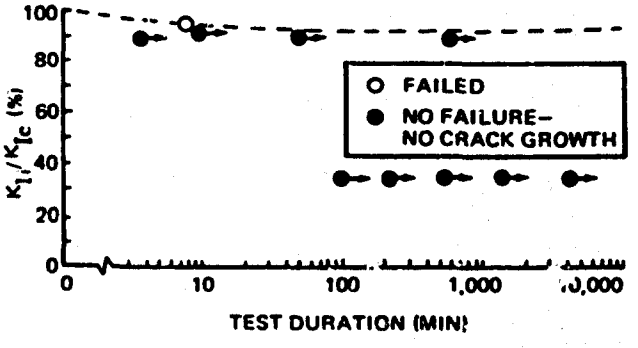

Fig. 13. Commercial alloy 300M tested in 90% relative humidity air.

Sustained load tests on heat J (300M) indicated a K_{Iscc} of 19.6 ksi$\sqrt{in}$. Furthermore, the crack growth rate was constant over a wide range of stress intensity (25 to 45 ksi$\sqrt{in}$.) and was 0.005 in./min. for stress intensity levels exceeding 45 ksi$\sqrt{in}$., the velocity was directly proportional to K. The difference in crack velocity kinetics between commercial and experimental alloys of similar alloy content and strength might be attributed to a finer grain size or the lower sulfur content in the commercial steel.

EFFECT OF COMPOSITION

The results obtained from the experimental alloys heat treated to the 280- to 300-ksi tensile strength range indicate that increasing the silicon content to above 1.5% does not improve K_{Iscc} but does retard crack growth rate. However, the results obtained from the surface-flawed specimens of commercial alloys suggest, at first sight, that silicon retards crack initiation. This apparently conflicting data can be reconciled by comparison of the residual element contents of the commercial heats. The sulfur and phosphorus contents of the air-melted 4340 were 0.019% and 0.021%, respectively, whereas the corresponding values for 300M (heat H) were 0.008% and 0.007%; the residual element content of vacuum degassed 4340 was in an intermediate position (Table I). It is therefore considered that the environmental crack growth resistance exhibited by the 300M steel can be primarily attributed to a lower residual element content.

CORRELATION WITH MICROSTRUCTURE

Baker et al. (11) have conducted thin-film electron microscopy studies on 4340 and 300M tempered over a wide temperature range. The microstructure of both alloys in the 260- to 300-ksi strength range consisted of a twinned martensite structure with a high dislocation density. Epsilon carbides were precipitated at the twin interfaces and martensite plate boundaries. As the tempering temperature was increased, the epsilon carbide was replaced by cementite and recovery and recrystallization of the martensite occurred. The investigators reported that the only effect of silicon was to retard these processes to higher tempering temperatures. Reisdorf (17) found that epsilon carbide in 300M steel contained a large proportion of silicon, whereas it was absent from the cementite formed at higher temperatures.

Since the present study indicated that silicon only retarded the crack velocity in the higher strength range, it would seem reasonable to associate this with the epsilon carbide. Polarization studies conducted by Steigerwald (13) have indicated that stress corrosion in 4340 steel can be attributed to a hydrogen embrittlement mechanism. Since fracture occurred along prior austenite boundaries, it might be postulated that stress corrosion cracking was associated with epsilon carbide particles at these boundaries and the presence of silicon retarded this process. Alternatively, the rate of hydrogen diffusion may be reduced by the silicon-containing epsilon carbides distributed at various sites within the microstructure and so retard the crack growth process.

In the strength range 230 to 240 ksi, the improvement in K_{Iscc} in the lower silicon content steels (Fig. 7) can be associated with the recovery processes and the change in carbide morphology, which would be more advanced than in the higher alloy content steels. The crack velocity, however, was essentially independent of silicon content (Table III). This possibly indicates that different microstructural features control threshold and crack velocity characteristics.

CRACK BRANCHING

Crack branching only occurred in steels that exhibited a region of constant velocity (Table III), and branching was observed to commence in this region. Furthermore, the steels tempered to 280-300 ksi did not branch and exhibited a linear dependence of crack velocity on stress intensity. These observations are in agreement with the work of other investigators (18,19), which indicated that a constant crack velocity is essential for crack branching. It has also been suggested

(18) that a critical stress intensity must be achieved before branching can occur; this was observed in this study. These crack branching observations are discussed further elsewhere (20).

COMPARISON WITH UNNOTCHED DATA

Unnotched bent beam tests conducted by Dreyer and Gallaugher (21) have indicated that silicon is beneficial to stress corrosion resistance. In these tests, 300M and 4340 specimens were loaded in bending to a predetermined fraction of the yield strength and subjected to alternate immersion in sodium chloride solution. The time to failure was measured as a function of applied stress level. Tiner and Gilpin (22) have shown that the failure process in such tests can be divided into three stages:

1. Pit formation and growth
2. Stress corrosion crack propagation
3. Rapid brittle fracture

The time occupied by the first stage depends on the surface finish; size and distribution of inclusions, carbides, and other discontinuities; and pitting characteristics of the alloy. Presumably, stress corrosion crack initiation occurs when the pit depth and acuity are sufficient for the stress intensity level to exceed K_{Iscc}. Provided that a sharp pit is formed, the critical depth for crack initiation will be given by:

$$S\left(\frac{K_{Iscc}}{\sigma_{ys}}\right)^2 = d_{CRIT} \qquad (2)$$

where σ_{ys} = yield stress
d_{CRIT} = pit depth
S = a factor determined by loading conditions and pit shape

Hence, for similar loading conditions, the critical pit depth for two alloys will be proportional to the square of their K_{Iscc} values. Assuming equal rates of pitting for 4340 and 300M steels, the duration of stage 1 should be similar for both steels. However, as Brown (23) has pointed out, the rate of pitting can be much slower than stress corrosion crack velocity. Therefore, small differences in K_{Iscc} between the two steels, for example due to a slight variation in residual element content, could lead to a very significant difference in the time required to achieve critical pit depth.

The duration of the second stage will depend upon the relationship between stress intensity and velocity, the rate of change of stress intensity with respect to crack length, and the fracture toughness. The latter is also influenced by the stress state (plane stress or plane strain). The velocity data obtained in the present study indicate that the duration of this stage will be longer in 300M than in 4340 and, hence, would contribute to the observations made by Dreyer and Gallaugher (21).

A FRACTURE TOUGHNESS CONSIDERATION

Considerable emphasis has been placed on improving fracture toughness in alloy systems. Because of this, it is interesting to consider the results obtained from the experimental heats containing 0.09% and 0.54% silicon tempered to 280-300 ksi. The latter steels had different fracture toughness values (74 and 55 ksi$\sqrt{in.}$, respectively), but the times to failure were comparable for a similar initial stress intensity level (Fig. 11). Examination of the crack velocity curves (Fig. 10) explains this observation. The crack velocity of the lower silicon steel at stress intensity levels above 55 ksi$\sqrt{in.}$ was so rapid that the additional crack growth required to reach critical length in the tougher steel occupied an insignificant amount of time. Under these circumstances, the improved fracture toughness would not improve service performance.

CONCLUSIONS

1. Additions of silicon of up to 2.15% to 4340 steel did not increase the threshold stress intensity parameter K_{Iscc} in the 280- to

300-ksi tensile strength range. However, the stress corrosion crack velocity was significantly retarded when the silicon content exceeded 1.5%.

2. Tempering to the 230- to 240-ksi tensile strength range improved K_{Iscc}. This was most apparent in the steels containing less than 1.5% silicon in which the tempering reactions were more advanced than those of the higher silicon content steels.

3. The crack velocity was directly proportional to stress intensity in the 280- to 300-ksi tensile strength range. For a tensile strength range of 230 to 240 ksi, the crack velocity was constant over a wide range of stress intensity.

4. Reducing the sulfur and phosphorus content of low-alloy, high-strength steels enhances the crack growth resistance.

ACKNOWLEDGMENTS

The author would like to thank A. M. Ross for assistance with the stress corrosion testing, and J. C. McMillan for permission to include his previously unpublished data obtained from surface-flawed specimens.

REFERENCES

1. C. H. Shih, B. L. Averbach, and M. Cohen, "Some Effects of Silicon on the Mechanical Properties of High Strength Steels," *Trans ASM*, 1956, *48*, p. 86

2. C. J. Alstetter, M. Cohen, and B. F. Averbach, "Effect of Silicon on the Tempering of AISI 43XX Steels," *Trans ASM*, 1962, *55*, p. 287

3. W. L. Holshouser, "Failure in Aircraft Parts Made of Ultra High Strength Steels," *ASM Metals Eng Quarterly*, August 1964, *4*, p. 8

4. R. I. Ault, "High Strength Steels," Report No. AFML-TR-65-29, *Proc. Air Force Materials Symposium*, Wright-Patterson Air Force Base, May 1965

5. R. P. Wei, "Fracture Toughness Testing in Alloy Development," *Fracture Toughness Testing and Its Applications*, ASTM, STP 381, 1965, p. 279

6. J. H. Gross, "The New Development of Steel Weldments," *Welding Journal*, 1968, *47*, p. 241s

7. W. F. Brown and J. E. Srawley, *Plane Strain Crack Toughness Testing of High Strength Metallic Materials*, ASTM, STP 410, 1966

8. B. F. Brown and C. D. Beacham, "A Study of the Stress Factor in Stress Corrosion Cracking," *Corrosion Science*, 1965, *5*, p. 745

9. B. F. Brown, "A New Stress Corrosion Cracking Test for High Strength Alloys," *ASTM Matls Res and Stds*, 1966, *66*, p. 129

10. G. R. Irwin, "Crack Extension Force for a Part-Through Crack in a Plate," *Trans ASME*, 1962, *29*, (4), p. 651

11. A. J. Baker, F. J. Lauta, and R. P. Wei, "Relationships Between Microstructure and Toughness in Quenched and Tempered Ultra High Strength Steels," *Structure and Properties of Ultra High Strength Steels*, ASTM, STP 370, 1965, p. 1

12. J. L. Guthrie, *High Strength Steel Evaluation for Supersonic Aircraft*, Boeing Document D6A10093-2, Commercial Supersonic Transport Program Phase II-C Report on Contract FA-SS-66-S, March 1967

13. W. D. Benjamin and E. A. Steigerwald, *Stress Corrosion Cracking Mechanisms in Martensitic High Strength Steels*, Technical Report AFML-TR-67-98, Wright-Patterson Air Force Base, 1967

14. H. H. Johnson and A. M. Willner. "Moisture and Stable Crack Growth in a Higl Strength Steel." *Applied Matls Res.* 1965. *4.* p. 34

15. C. S. Carter. *Crack Extension in Several High Strength Steels Loaded in 3.5% Sodium Chloride Solution.* Boeing Document D6-19770. 1967 (available from Defense Documentation Center)

16. G. R. Irwin. "Structural Aspects of Brittle Fracture." *Applied Matls Rcs.* 1964, 3. p. 65

17. B. G. Reisdorf. "The Tempering Characteristics of Some 0.4% Carbon Ultra High Strength Steels." *Trans AIME.* 1963. *227.* p. 1334

18. A. B. J. Clark and G. R. Irwin. "Crack Propagation Behaviors." *Expt Mechs.* 1966. *23.* p. 321

19. S. Mostovoy. R. G. Lingwall. and E. J. Ripling. private communication to The Boeing Company. December 1968

20. C. S. Carter. "Stress Corrosion Crack Branching in High Strength Steels." Boeing Document D6-23871. 1969 (available from Defense Documentation Center)

21. G. A. Dreyer and W. G. Gallaugher. *Investigation of Susceptibility of High Strength Martensitic Steel Alloys to Stress Corrosion.* Technical Documentary Report No. ASD-TDR-62-876. Wright-Patterson Air Force Base. 1962

22. N. A. Tiner and C. B. Gilpin. "Microprocesses in Stress Corrosion Cracking of Martensitic Steels." *Corrosion.* 1966. *22.* p. 271

23. B. F. Brown. "Stress Corrosion Cracking and Corrosion Fatigue of High Strength Steels." *Problems in the Load Carrying Applications of High Strength Steels.* DMIC Report No. 210. 1964. p. 91

Unclassified
Security Classification

DOCUMENT CONTROL DATA - R & D

(Security classification of title, body of abstract and indexing annotation must be entered when the overall report is classified)

1. ORIGINATING ACTIVITY (Corporate author)	2a. REPORT SECURITY CLASSIFICATION
The Boeing Company Commercial Airplane Division Renton, Washington	2b. GROUP

3. REPORT TITLE

The Effect of Silicon on the Stress Corrosion Resistance of Low-Alloy, High-Strength Steels

4. DESCRIPTIVE NOTES (Type of report and inclusive dates)

Research Report

5. AUTHOR(S) (First name, middle initial, last name)

C. S. Carter

6. REPORT DATE	7a. TOTAL NO. OF PAGES	7b. NO. OF REFS
March 1969	13	23

8a. CONTRACT OR GRANT NO.	9a. ORIGINATOR'S REPORT NUMBER(S)
N00014-66-C0365 b. PROJECT NO. c. d.	Boeing Document D6-23872 9b. OTHER REPORT NO(S) (Any other numbers that may be assigned this report)

10. DISTRIBUTION STATEMENT

Reproduction in whole or in part is permitted by the United States Government.
Distribution of this document is unlimited.

11. SUPPLEMENTARY NOTES	12. SPONSORING MILITARY ACTIVITY
	Advanced Research Projects Agency, Department of Defense

13. ABSTRACT

The effect of five levels of silicon, within the range 0.09 to 2.15 wt %, on the stress corrosion resistance of 4340 steel was established in 3.5% sodium chloride solution for two tensile strength ranges (280 to 300 ksi and 230 to 240 ksi). At the higher strength range, the threshold stress intensity was independent of silicon content, but the stress corrosion crack velocity was significantly retarded when the silicon content exceeded 1.5 wt %. At the 230- to 240-ksi strength range, steels containing less than 1.5 wt % silicon exhibited a higher K_{Iscc} threshold than steels of higher silicon content. Strength level had a significant effect on crack velocity characteristics.

DD FORM 1 NOV 65 1473

Unclassified
Security Classification

14 KEY WORDS	LINK A		LINK B		LINK C	
	ROLE	WT	ROLE	WT	ROLE	WT
Stress corrosion						
Alloy content						
High-strength steels						
Fracture mechanics						
Crack velocity						